

07.2;07.3

Photodetectors with the long-wavelength cutoff of $2.4\ \mu\text{m}$ based on metamorphic InGaAs/InP heterostructures grown by metal-organic vapor-phase epitaxy

© N.A. Kalyuzhnyy¹, S.S. Kizhaev², S.A. Mintairov¹, A.A. Pivovarova¹, R.A. Salii¹, A.V. Chernyaev^{2,3}

¹ Ioffe Institute, Saint-Petersburg, Russia

² „LED Microsensor NT“ LLC, Saint-Petersburg, Russia

³ Budenny military communication academy, Saint-Petersburg, Russia

E-mail: Nickk@mail.ioffe.ru

Received April 22, 2024

Revised May 8, 2024

Accepted May 8, 2024

The technique for growing metamorphic InGaAs buffer layers on InP substrates was used to create photodetectors with the long-wavelength cutoff of $2.4\ \mu\text{m}$. Optical and electrical characteristics of photodetectors based on the InGaAs/InP metamorphic heterostructure and those of devices based on the GaInAsSb/GaSb isoperiodic system were compared. Instrumental applicability of the developed technique is confirmed by high reverse-bias photosensitivity and resistance of the photodetectors. The dark current values correlate with low density of threading dislocations in the photodetector active region assessed by transmission electron microscopy.

Keywords: photodetector, InGaAs/InP, metal-organic vapor-phase epitaxy, metamorphic layer, heterostructure.

DOI: 10.61011/TPL.2024.09.59144.19966

Photodetectors (PDs) of radiation with a wavelength exceeding $2\ \mu\text{m}$ are used in spectroscopy of a number of substances, e.g. hydrocarbons; this is important for medical diagnostics and controlling industrial production processes. PDs may also be used as thermophotovoltaic converters transforming waste heat generated in production cycles into electrical energy.

The use of quaternary solid solution $\text{Ga}_{1-x}\text{In}_x\text{As}_{1-y}\text{Sb}_y$ matched in lattice to the GaSb substrate is a conventional solution to the problem of manufacturing photoconverters for the wavelength range of $2.0\text{--}2.4\ \mu\text{m}$ [1,2]. However, the GaSb susceptibility to oxidation [3] makes it necessary to perform, prior to growing the layers, additional processing even of formally epi-ready GaSb- substrates. Also there are some technological difficulties in growing $\text{Ga}_{1-x}\text{In}_x\text{As}_{1-y}\text{Sb}_y$ solid solutions [4]. In addition, defect-induced recombination losses in PDs based on GaSb-containing solid solutions [5] increase the dark current density in such structures and reduce reproducibility of results.

An alternative can be GaInAs where variation in the third-group sublattice atom concentration makes it possible to obtain solid solutions with a radiation absorption edge in a wide spectral range, from near-IR to $3.6\ \mu\text{m}$. However, only solid solutions $\text{In}_x\text{Ga}_{1-x}\text{As}$ with the InAs mole fraction of 53% are isoperiodic with available semiconductor substrates (InP). PDs based on such a material [6] have a long-wavelength cutoff of $1.7\ \mu\text{m}$. Extension to the wavelength range of up to $2.4\ \mu\text{m}$ needs growing the $\text{In}_x\text{Ga}_{1-x}\text{As}$ solid solutions with the InAs mole fraction exceeding 80%, whose mismatch with the substrate reaches several percent. The problem may be solved by using the technique of metamorphic buffer layers (MBLs) whose task is transition from

the substrate lattice parameter to that of the photodetector active region by, e.g. smoothly or stepwise varying the lattice parameter. The main goal in designing MBLs is to prevent threading of misfit dislocations into the device active region.

The technique of the $\text{In}_x\text{Ga}_{1-x}\text{As}$ MBLs was largely developed aimed at GaAs substrates for creating the InGaAs subcell with the bandgap of $\sim 1\ \text{eV}$ in cascade solar photoconverters [7–9]. The authors of this study have previously developed a technique for growing by metal-organic vapor phase epitaxy (MOVPE) the $\text{In}_x\text{Ga}_{1-x}\text{As}$ MBLs on GaAs substrates [10,11] for PDs of the $1.02\text{--}1.06\ \mu\text{m}$ laser radiation, which demonstrate a record (50–55% [12, 13]) energy efficiency. In this paper, we elaborate the idea of applying the developed $\text{In}_x\text{Ga}_{1-x}\text{As}$ MBLs in adapting the technique of metamorphic growth on InP substrates for PDs with absorption edge of up to $2.4\ \mu\text{m}$. The difference from the previously developed MBL technique consists in introducing extra layers necessary for matching with the PD active region material that is the $\text{In}_{0.81}\text{Ga}_{0.19}\text{As}$ solid solution. Studies concerning the creation of such MBLs are poorly covered in literature. Paper [14] has reported MBE growth of the $\text{In}_x\text{Ga}_{1-x}\text{As}$ MBLs different in design and synthesis parameters; however, no information on the technique instrumental application has been demonstrated. Rather, there is no data on technological and design features of commercially available PDs with wavelengths of up to $2.4\ \mu\text{m}$ [6]. Paper [15] investigated the possibilities of growing $\text{In}_x\text{Ga}_{1-x}\text{As}$ structures on both GaAs and InP substrates through a buffer of another type, namely, based on the $\text{InAs}_{1-y}\text{P}_y$ layers.

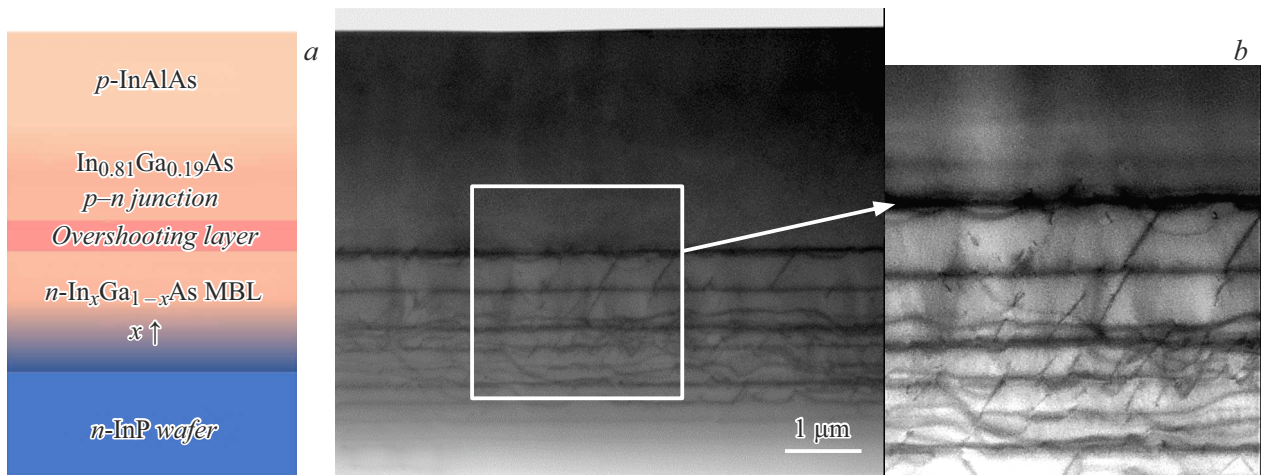


Figure 1. Schematic diagram (a) and STEM image (b) of the grown epitaxial InGaAs/InP PD heterostructure. The inset presents a zoomed part of the STEM- image containing the MBL top part, which demonstrates the overshooting layer and 60° threading dislocations.

Comparison of the main parameters of the developed InGaAs/InP PDs and commercial E2082 photodiodes

Parameter	InGaAs/InP	E2082
$I_{dark}, \mu A$ (-1000 mV)	18	160
$R_0, k\Omega$	3.6	2.6
$S, A/W$ (2200 nm)	0.83	0.89
NEP, $W \cdot Hz^{-1/2}$	$2.56 \cdot 10^{-12}$	$2.95 \cdot 10^{-12}$
$D^*, cm \cdot Hz^{1/2}/W$	$3.4 \cdot 10^{10}$	$3.1 \cdot 10^{10}$

The heterostructures were grown by MOVPE on the *n*-InP substrates from the Group 3 metal alkyls and arsine. The layers were doped with monosilane and bis(cyclopentadienyl)magnesium. The metamorphic buffer had a fixed-pitch stepped-composite profile and was terminated by an „overshooting“ layer [11]. After that, the PD active region was grown based on the *n*-type solid solution $In_{0.81}Ga_{0.19}As$ and *p*-type wide-bandgap semiconductor $In_{0.81}Al_{0.19}As$ that played also a role of a wide-bandgap heterostructure window (Fig. 1, a).

The grown heterostructures were examined by transmission electron microscopy and scanning transmission electron microscopy (STEM) with a JEOL JEM 2100 electron microscope. STEM allows demonstrating in one and the same image (Fig. 1, b) both the network of dislocations formed in MBL and small dislocation concentration in the „overshooting“ layer (its boundary is visible in the zoomed part of the STEM image, inset in Fig. 1, b), and also the absence of threading dislocations in the entire photoactive part of the heterostructure. The STEM image demonstrates inclined 60° dislocations characteristic of the metamorphic growth with strong lattice mismatch [16], which form during threading high-density edge misfit dislocations at the MBL boundaries. Buffer layers acting as a source of threading dislocations promote relaxation of stresses in the growing layer

due to nucleation of edge dislocations at the boundaries and prevent penetration of dislocations into the photoactive region. A detailed study of various heterostructure regions at the interface between MBL and photoactive region gave the dislocation density estimate of $< 5 \cdot 10^6 cm^{-2}$. Although transmission electron microscopy provides only estimative characteristics of dislocations, this result correlates with low leakage currents demonstrated on devices fabricated based on epitaxial metamorphic heterostructures (see the Table).

Heterostructure-based PDs with the sensitive area 1 mm in diameter were fabricated by conventional photolithography and wet chemical etching. The Au–Ge–NiAu material system was used to make contacts on the side of the *n*-InP substrate, while the Cr–Au–NiAu system was used for the *p*-InAlAs top layer. The sensitive pad was formed on the heterostructure epitaxial side. No antireflective coatings were used. The photodetector chips were mounted on the TO-18 casing.

Spectral and current-voltage characteristics (Fig. 2) of the fabricated PDs were measured. The electrical circuit contained a voltage sweep generator and load resistor for measuring electric current (in series with the sample). Spectral setup MDR-41 used in this study was designed for the visible and IR radiation range of 0.4–10 μm . The main modules were: source of black (gray) body radiation, $T = 1150^\circ C$; monochromator MDR-41 with a set of diffraction gratings of 150 to 1500 mm^{-1} ; two mirror condensers (project the source image onto the monochromator input slit and from the monochromator output slit onto the photodetector); light flux modulator. The photodetector dark current and resistance R_0 were measured in the manual mode with direct current by using a circuit where the photodetector was connected in series with reference resistance R_{ref} 1 k Ω in nominal. Voltage was measured from both the photodetector and reference resistance (for measuring electric current through the photodetector). Electrical capacitance of photodetectors

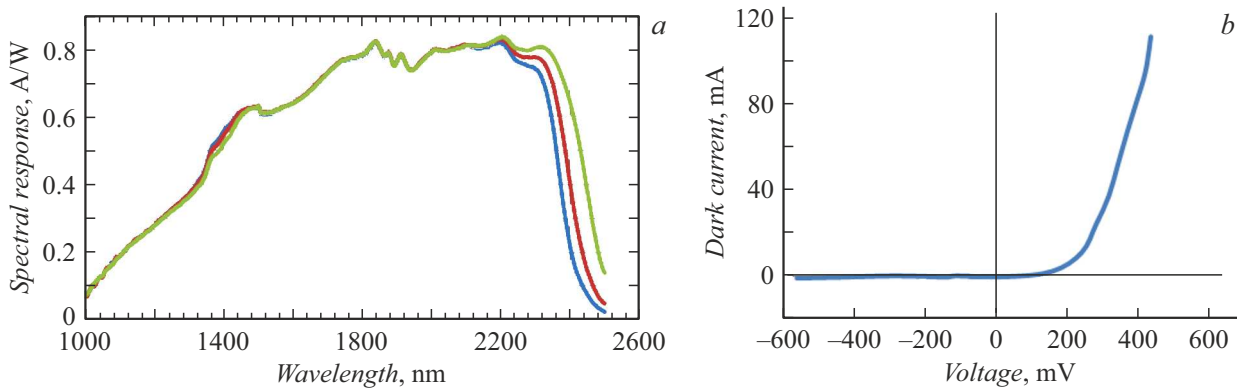


Figure 2. Photoresponse spectra for a set of three samples (a) and typical current-voltage characteristic (b) of PD based on metamorphic epitaxial heterostructures InGaAs/InP.

was determined using a precise metering device. All the measurements were performed at room temperature.

Based on the measurements, photodetector parameters were calculated: noise equivalent power (NEP) and specific detection ability D^* related to the wavelength of 2.2 μm. Calculations were performed via formulae

$$\text{NEP} = \frac{\sqrt{4k_B T}}{S\sqrt{R_0}}, \quad (1)$$

$$D^* = \frac{\sqrt{A}}{\text{NEP}}, \quad (2)$$

where S is the sensitivity, R_0 is the photodetector resistance at near-zero reverse bias (−10 mV), A is the area of the photodetector sensitive area, T is the temperature, k_B is the Boltzmann constant.

Measurements and calculations for photodetectors based on the p -InGaAs/ n -InP PD epitaxial structure are presented in the table jointly with those for commercial E2082 photodiodes [17] with the long-wavelength cutoff of 2.4 μm fabricated based on the lattice-matched heterostructure p -AlGaAsSb/GaInAsSb/ n -GaSb grown by liquid-phase epitaxy. At the similar spectral sensitivity, the best parameter R_0 is exhibited by PDs developed based on metamorphic heterostructures. The increased PD resistance at the reverse bias, as well as lower dark current I_{dark} , points at lower leakage currents (even compared to a fully isoperiodic structure). As shown in the correlation comparison [13], this means that the MBL technique allows avoiding the dislocation threading into the active region, which would cause the dominance of the „leakage“ tunnel-trap mechanism of the current flow in the p - n junction.

High R_0 allows improving utilitarian parameters NEP and D^* (as follows from expressions (1) and (2)). Thus, comparison of characteristics of PDs based on different material systems (isoperiodic and mismatched ones) shows that there has been developed a technological basis for creating metamorphic epitaxial heterostructures promising for photodetectors with the long-wavelength cutoff of 2.4 μm.

Acknowledgements

The authors are grateful to V.N. Nevedomsky for examining the samples with a transmission electron microscope.

Conflict of interests

The authors declare that they have no conflict of interests.

References

- [1] E.V. Kunitsyna, I.A. Andreev, G.G. Konovalov, A.A. Pivovarova, N.D. Il'inskaya, Yu.P. Yakovlev, Ya.Ya. Ponurovskii, A.I. Nadezhdinskii, A.S. Kuzn'ichev, D.B. Stavrovskii, M.V. Spiridonov, *Semiconductors*, **56** (5), 351 (2022). DOI: 10.21883/SC.2022.05.53432.9813.
- [2] A.N. Imenkov, B.E. Zhurtanov, A.P. Astakhova, K.V. Kalinina, M.P. Mikhailova, M.A. Sipovskaya, N.D. Stoyanov, *Tech. Phys. Lett.*, **35** (1), 67 (2009). DOI: 10.1134/S1063785009010209.
- [3] Ch. Giesen, M. Heuken, F. Dimroth, A. Bett, T. Hannapel, Z. Kollonitsch, K. Möller, M. Seip, J. Koch, A. Greiling, *AIP Conf. Proc.*, **738** (1), 267 (2004). DOI: 10.1063/1.1841903
- [4] T. Burger, C. Sempere, B. Roy-Layinde, A. Lenert, *Joule*, **4** (8), 1660 (2020). DOI: 10.1016/j.joule.2020.06.021
- [5] C.A. Wang, *AIP Conf. Proc.*, **738** (1), 255 (2004). DOI: 10.1063/1.1841902
- [6] www.hamamatsu.com [Electronic source].
- [7] F. Dimroth, W. Guter, J. Schöne, E. Welsler, M. Steiner, E. Oliva, A. Wekkeli, G. Siefert, S.P. Philips, A.W. Bett, in *2009 34th IEEE Photovoltaic Specialists Conf. (PVSC)* (IEEE, 2009), p. 001038. DOI: 10.1109/pvsc.2009.5411199
- [8] T. Takamoto, H. Washio, H. Juso, in *2014 IEEE 40th Photovoltaic Specialist Conf. (PVSC)* (IEEE, 2014), p. 0001. DOI: 10.1109/PVSC.2014.6924936
- [9] J.F. Geisz, R.M. France, K.L. Schulte, M.A. Steiner, A.G. Norman, H.L. Guthrey, M.R. Young, T. Song, T. Moriarty, *Nat. Energy*, **5**, 326 (2020). DOI: 10.1038/s41560-020-0598-5
- [10] S.A. Mintairov, V.M. Emelyanov, D.V. Rybalchenko, R.A. Sali, N.K. Timoshina, M.Z. Shvarts, N.A. Kalyuzhnyy, *Semiconductors*, **50** (4), 517 (2016). DOI: 10.1134/S1063782616040163.

- [11] N.A. Kalyuzhnyy, S.A. Mintairov, A.M. Nadtochiy, V.N. Nevedomskiy, D.V. Rybalchenko, M.Z. Shvarts, *Electron. Lett.*, **53** (3), 173 (2017). DOI: 10.1049/el.2016.4308
- [12] N.A. Kalyuzhnyy, V.M. Emelyanov, S.A. Mintairov, M.V. Nahimovich, R.A. Salii, M.Z. Shvarts, *AIP Conf. Proc.*, **2298** (1), 030001 (2020). DOI: 10.1063/5.0032903
- [13] N.A. Kalyuzhnyy, V.M. Emelyanov, V.V. Evstropov, S.A. Mintairov, M.A. Mintairov, M.V. Nahimovich, R.A. Salii, M.Z. Shvarts, *Solar Energy Mater. Solar Cells*, **217**, 110710 (2020). DOI: 10.1016/j.solmat.2020.110710
- [14] E.I. Vasilkova, E.V. Pirogov, M.S. Sobolev, E.V. Ubyivovk, A.M. Mizerov, P.V. Seredin, *Kondensirovannye sredy i mezhfaznye granitsy*, **25** (1), 20 (2023). DOI: 10.17308/kemf.2023.25/10972 (in Russian)
- [15] K.L. Schulte, D.J. Freidman, T. Dada, H.L. Guthrey, E.W. Costa, E.J. Tervo, R.M. France, J.F. Geisz, M.A. Steiner, *Adv. Energy Mater.*, **14** (10), 2303367 (2024). DOI: 10.1002/aenm.202303367
- [16] D.C. Houghton, D.D. Perovic, J.-M. Baribeau, G.C. Weatherly, *J. Appl. Phys.*, **67** (4), 1850 (1990). DOI: 10.1063/1.345613
- [17] www.lmnst.com [Electronic source].

Translated by EgoTranslating